Electronic Supplementary Information

Metal oxide- and N-codoped carbon nanosheets: facile synthesis derived from MOF nanofibers and their application in oxygen evolution

Xuan Kuang*, Zhiling Wang, Xu Sun, Yong Zhang and Qin Wei*

School of Chemistry and Chemical Engineering, University of Jinan, Jinan 250022, P. R. China.

Key Laboratory of Interfacial Reaction & Sensing Analysis in Universities of Shandong; Shandong Provincial Key Laboratory of Fluorine Chemistry and Chemical Materials, Jinan 250022, P. R. China.

Corresponding author e-mail: chm_kuangx@ujn.edu.cn；chm_weiq@ujn.edu.cn

Experimental details

Material. Metal salts and other reagents were purchased from Sigma-Aldrich (Shanghai, China). Nafion solution (5 wt %) was purchased from DuPont, Ltd. Ultrapure water (18.2MU cm) was obtained from a Water Purification System (Labconco Corporation, Kansas City, USA). All reagents were of analytical grade and used without further purification.

Structural Characterization. The morphology, structure, and elemental distribution was characterized using field-emission scanning electron microscope (FESEM, FEI QUANTA FEG250, FEI Company, USA). Powder X-ray diffraction data (PXRD) for crystal structure characterization were recorded on a Bruker SMART APEX CCD-based diffractometer (Cu Kα radiation, λ = 1.5418 Å). Chemical compositions of materialswere studied by energy dispersive X-ray spectrometry (EDXS) with an Oxford INCA Energy X-MAX-50 X instrument.X-ray photoelectron spectroscopy (XPS) measurements were conducted on a PHI 5000 VersaProbe (UlVAC-PHI Company, Japan), and curve fitting of elemental fine spectra were performed using 20% Gaussian-Lorentzian peak shape.

Material Preparation

Synthesis of Cu(II)-Asp@Co(II) nanofibers with Cu(II)/ Co (II) ratio of 1:1. An aqueous solution

(18 mL) of $Cu(NO_3)_2{\cdot}3H_2O$ (1.25 mmol) and $Co(NO_3)_2{\cdot}6H_2O$ (1.25 mmol) was mixed with an aqueous solution (2 mL) of *l*-aspartic acid (0.41 mmol) and NaOH (0.58 mmol) at room temperature. The mixture turned turbid immediately, and allowed to stand at room temperature for 1 h, and filtered. The obtained precipitate was washed with ethanol and dried at 60 ^{o}C. Cu(II)-Asp@Co(II) powder was obtained in a high yield (87%).

Synthesis of Cu(II)-Asp@Co(II) nanofibers with Cu(II)/Co (II) of other ratio. An aqueous solution (18 mL) of $Cu(NO_3)_2{\cdot}3H_2O$ and $Co(NO_3)_2{\cdot}6H_2O$ (2.5 mmol total) with different ration was mixed with an aqueous solution (2 mL) of *l*-aspartic acid (0.41 mmol) and NaOH (0.58 mmol) at room temperature. The mixture turned turbid, and allowed to stand at at room temperature for 1 h, and filtered. The obtained precipitate was washed with ethanol and dried at 60 ^{o} C. Cu(II)-Asp@Co(II) powder was obtained in a high yield.

Synthesis of [Cu(II)-Asp$(H_2O)_x]_n$] nanofibers. $Cu(NO_3)_2{\cdot}3H_2O$ (2.5 mmol) was mixed with an aqueous solution (2 mL) of *l*-aspartic acid (0.41 mmol) and NaOH (0.58 mmol) at room temperature. The mixture turned turbid immediately, and allowed to stand at room temperature for 1 h, and filtered. The obtained precipitate was washed with ethanol and dried at 60 ^{o} C. [Cu(II)-Asp$(H_2O)_x]_n$]powder was obtained.

Synthesis of Co(II)-Asp fibers. Numerous attempts to synthesize the Co(II)-Asp fibers without Cu(II) ions by varing the ratios and concentrations of Co(II) ions/Asp, pH values, reacting time and temperatures, have failed.

Pyrolysis of Cu(II)-Asp@Co(II) and [Cu(II)-Asp$(H_2O)_x]_n$] nanofibers. The Cu(II)-Asp@Co(II) and [Cu(II)-Asp$(H_2O)_x]_n$]nanofibers were transferred into in a tube furnace and then heated up to design temperature at a rate of 5 °C min^{-1} and kept for 2 h in air, then being cooled to RT at a ramp of 2 °C·min^{-1}. The resultant product for Cu(II)-Asp@Co(II) with Cu(II)/Co(II) ratio of 1:1 at 300 °C was denoted as NC@CoO/CuO, the one from [Cu(II)-Asp(H_2O)x]n] nanofibers at 300 °C was denoted as NC@ CuO. Other products for Cu(II)-Asp@Co(II) with Cu(II)/Co(II) ratio of n/m at 300 °C were denoted as NC@CoO/CuO-n/m.

Preparation of NC nanosheets without CoO and CuO. The as-prepared NC@CoO/CuO-1/1 nanosheets were soaked in dilute hydrochloric acid, then washed using water and dried.

Electrochemical Measurements

The electrocatalytic activity was evaluated on a CHI660B electrochemical workstation

(Shanghai Chenhua Limited, China) with a three-electrode system at room temperature (RT). A glassy carbon (GC) disk electrode (4mm in diameter) served as the support for the working electrode. Before the coating of catalyst, the GC electrode was polished with aqueous alumina suspension, followed by rinsing with distilled water and ultrapure water, respectively, and dried at RT. A homogeneous catalyst suspension was prepared by dispersing 4.0 mg of catalyst in 1 mL of the solution containing 0.72 mL of water, 0.25 mL of isopropanol and 30 μL of Nafion solution (5 wt%), followed by ultrasonication for 15 min. Then, 6 μL of the suspension was pipetted using a micropipettor on the GC surface. The Ag/AgCl (filled with 3 M KCl), Pt wire and a glass carbon disk of 4 mm diameter were used as the reference electrode and counter electrode, respectively. The converted potentials were referenced to a reversible hydrogen electrode (RHE):

$E_{RHE} = E_{Ag/AgCl} + (0.1976+0.059\ pH)\ V$

where $E_{Ag/AgCl}$ is the experimentally measured potential against Ag/AgCl reference, pH is 13.7 (in 0.5 M KOH).

Linear sweep voltammetry was recorded in 0.5 M KOH at a scan rate of 5 $mV \cdot s^{-1}$ to obtain the polarization curves. The thermodynamic potential for $4OH^- \rightarrow 2H2O + O2 + 4e^-$:

$E°(OH^-/O_2) = 1.228 - 0.059pH$

The corrected overpotential, $\eta(V) = E_{Ag/AgCl} - [1.228 - (0.1976+0.059\ pH) = E_{RHE} - 1.228\ V$

Electrochemical impedance spectroscopy (EIS) analysis was carried out with frequency from 0.1 to 1000 kHz with an amplitude of 10 mV at the open-circuit voltage. The long-term stability tests were performed by the polarization curve test after continuous linear sweep voltammetry scans between 0.0 and 0.6 V (vs. Ag/AgCl) in 0.5 M KOH) at a sweep rate of 50 $mV \cdot s^{-1}$.

Additional Results

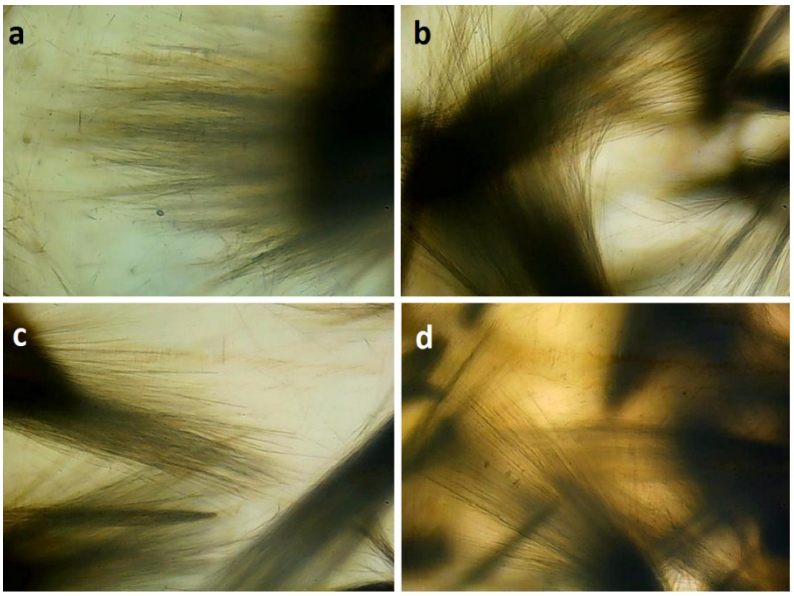

Fig.S1. Optical microscope images of (a) [Cu(II)-Asp$(H_2O)_x]_n$] and Cu(II)-Asp@Co(II) nanofibers with Cu(II)/Co(II) ratios of (b) 7:3 , (c) 1:1 and (d) 3:7, magnified 500 times.

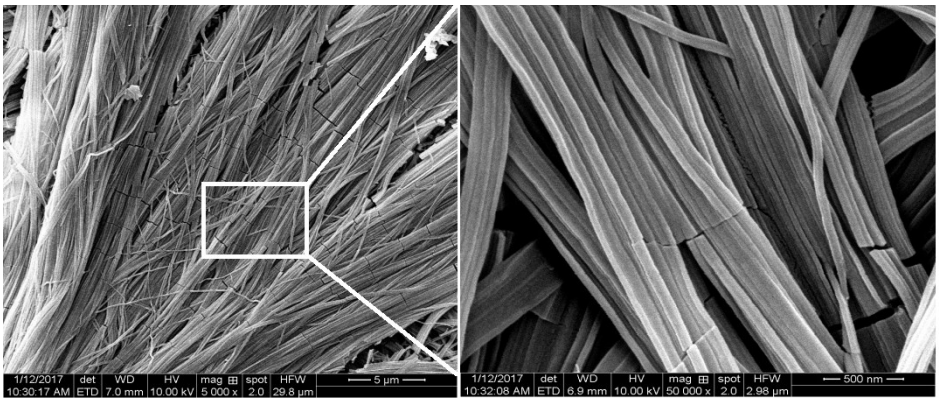

Fig. S2. High magnification FE-SEM images of Cu(II)-Asp@Co(II) nanofibers with Cu(II)/Co(II) ratio of 1:1.

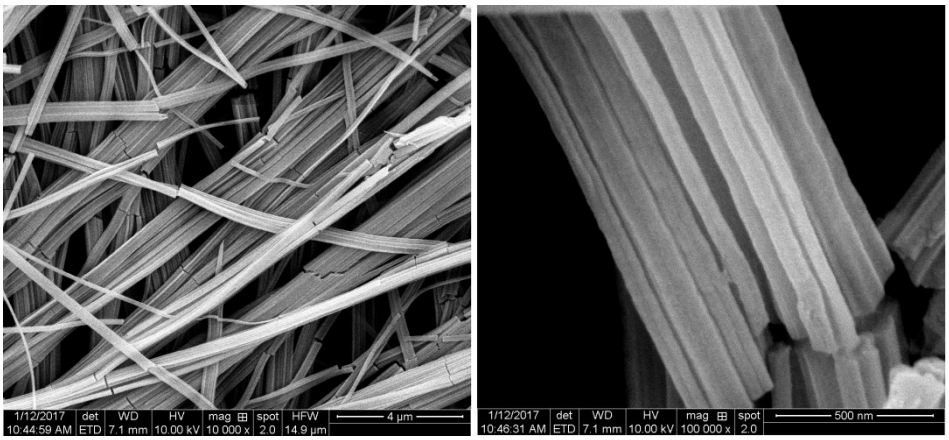

Fig. S3. High magnification FE-SEM images of [Cu(II)-Asp$(H_2O)_x]_n$] nanofibers without Co(II) ions.

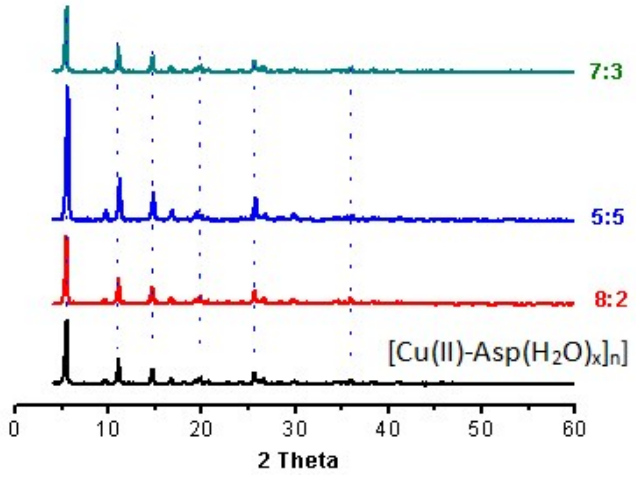

Fig. S4. XRD of [Cu(II)-Asp$(H_2O)_x]_n$] nanofibers without Co(II) ions (a) and Cu(II)-Asp@Co(II) nanofibers with Cu(II)/Co(II) ion ratios of (b)8:2, (c) 5:5 (1:1)and(d) 7:3 , respectively.

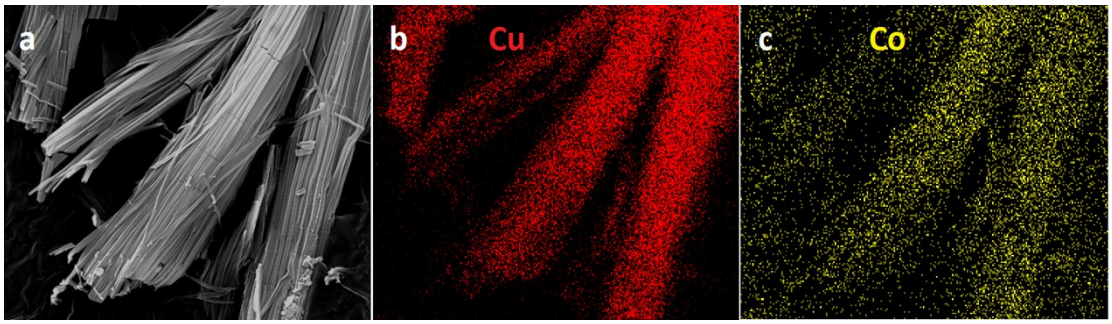

Fig. S5. Elemental mappings of Cu(II)-Asp@Co(II) nanofibers (a) given by energy dispersive spectroscopy (EDS)for Cu (b) and Co (c) elements with Cu(II)/Co(II) ion ratio of 1:1.

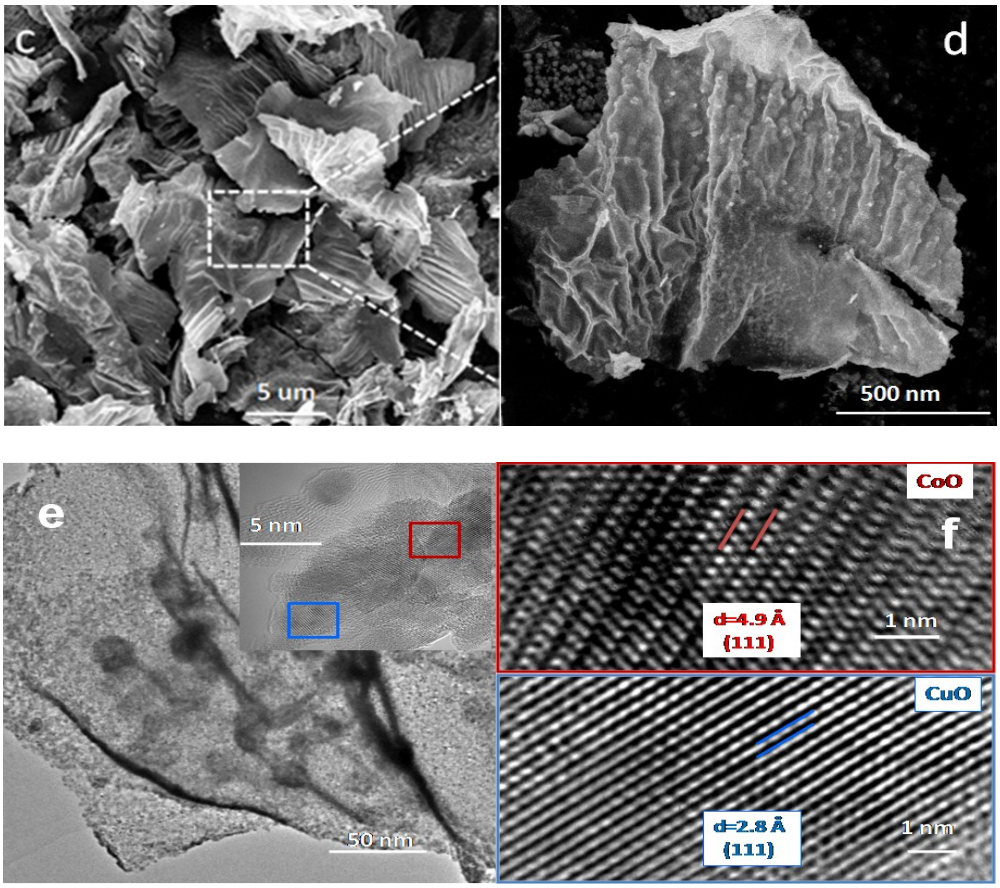

Fig. S6. High magnification images of FE-SEM (a,b) and HRTEM (c,d) of NC@CoO/CuO derived from pyrolysis of Cu(II)-Asp@Co(II) nanofibers with Cu(II)/Co(II) ion ratio of 1:1 at 300 ^{o}Cfor 2 h.

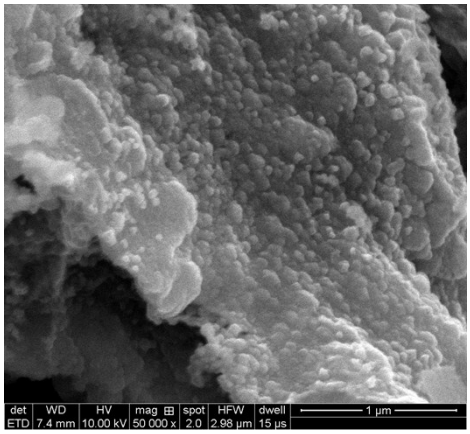

Fig. S7. High magnification FE-SEM images of NC@CuO derived from pyrolysis of $[Cu(II)(Asp)(H_2O)_x]_n$ nanofibers at 300 ^oC for 2 h.

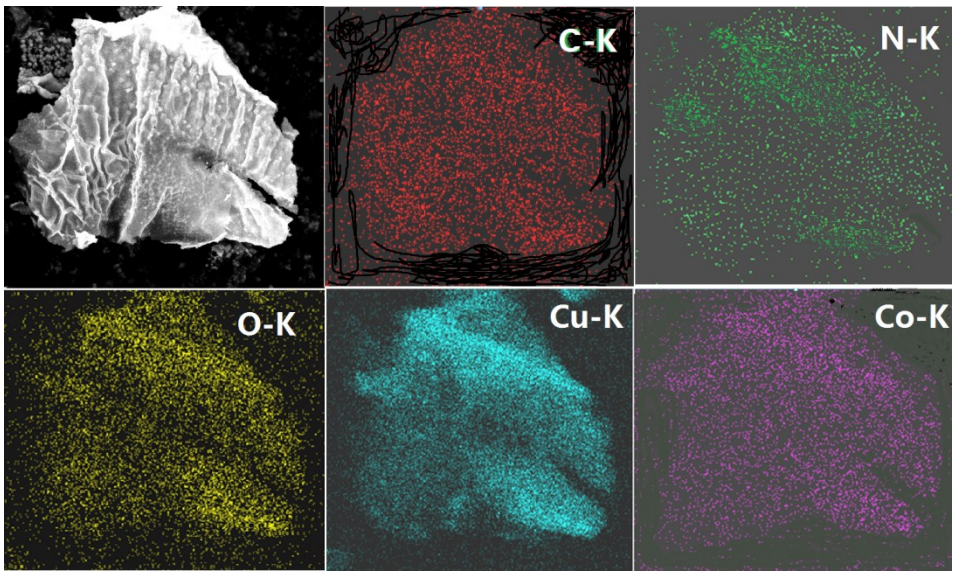

Fig. S8. Elemental mapping results of the microstructures in NC@CoO/CuO by SEM-EDS.

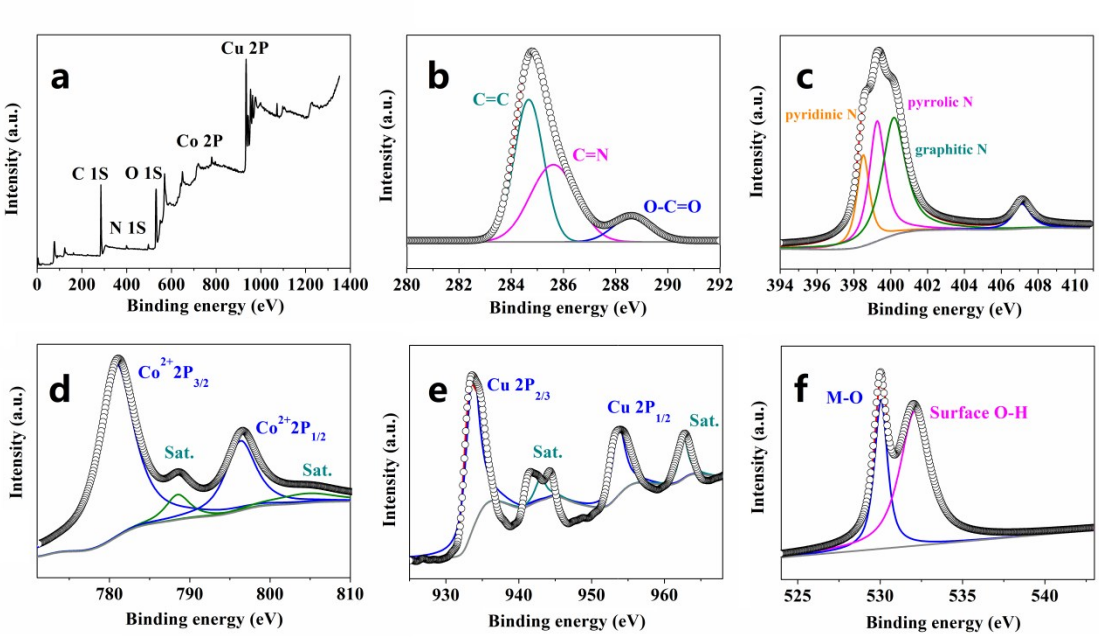

Fig.S9. XPS survey of as-prepared NC@CoO/CuOnanosheets,(a) survey spectrum, (b) C 1S, (c) N1S, (d) Co 2P, (e) Cu 2P and (f) O 1s spectra.

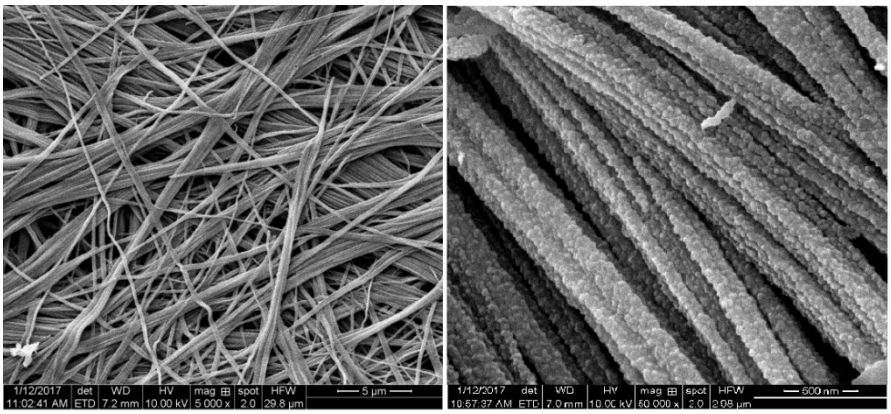

Fig. S10. High magnification FE-SEM images of material derived from pyrolysis of Cu(II)-Asp@Co(II) nanofibers with Cu(II)/Co(II) ratio of 1:9 at 300 ^{o}C for 2 h.

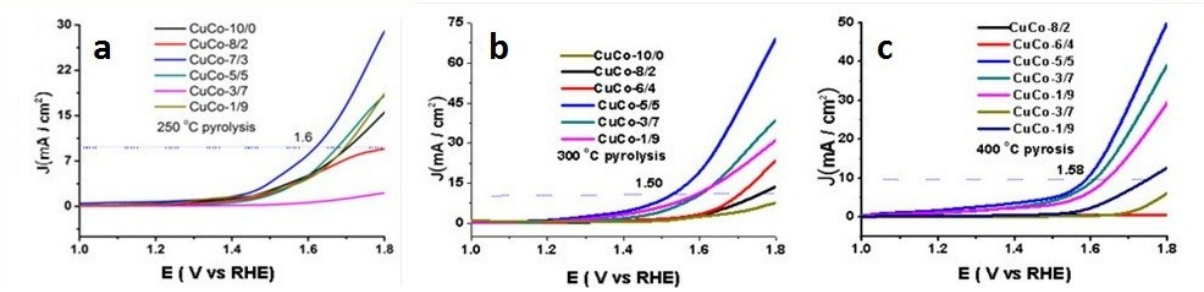

Fig. S11. Polarization curves of materials derived from pyrolysis of Cu(II)-Asp@Co(II) nanofiberswith Cu(II)/Co(II) of different ratioat 250 °C, 300 °C and 400 °C.

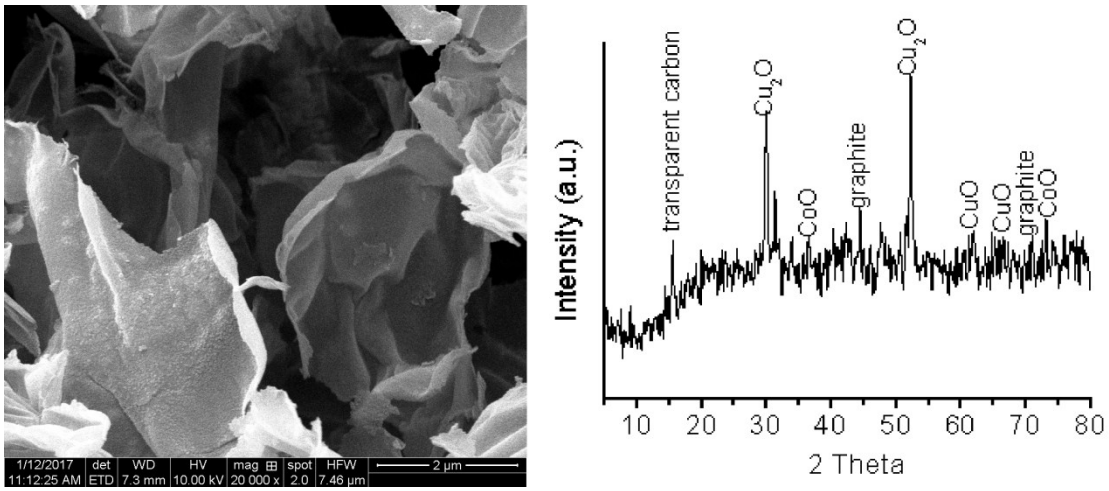

Fig. S12. FE-SEM images and XRD patterns of the materials obtained from pyrolysis of Cu(II)-Asp@Co(II) nanofibers with Cu(II)/Co(II) of 1:1 at 250 °C.

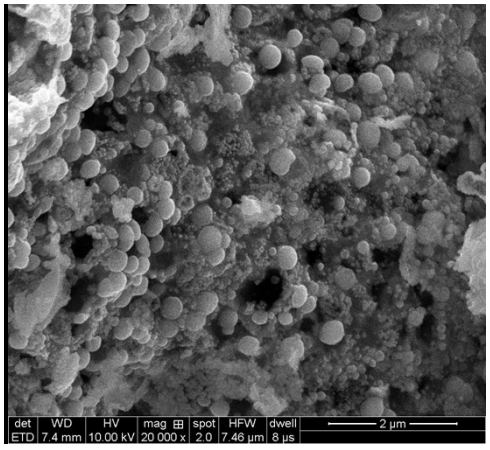

Fig. S13. FE-SEM images of material derived from pyrolysis of Cu(II)-Asp@Co(II) nanofibers with Cu(II)/Co(II) ratio of 1:1 at 400 °C for 2 h.

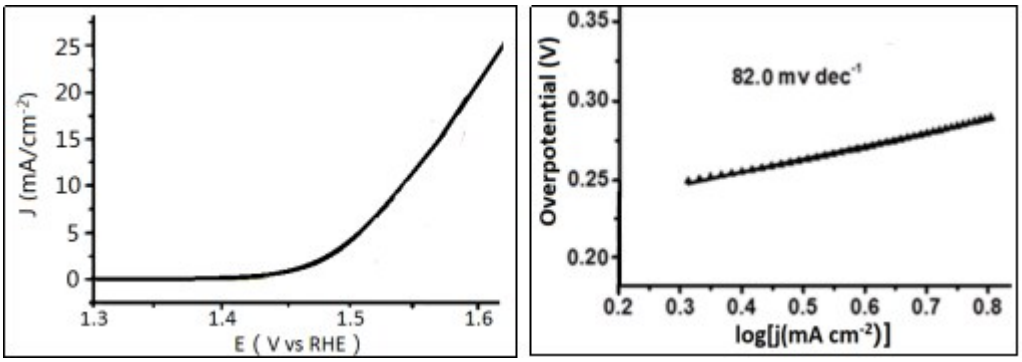

Fig. S14.Polarization curves and Tafel slope of RuO_2 for OER.

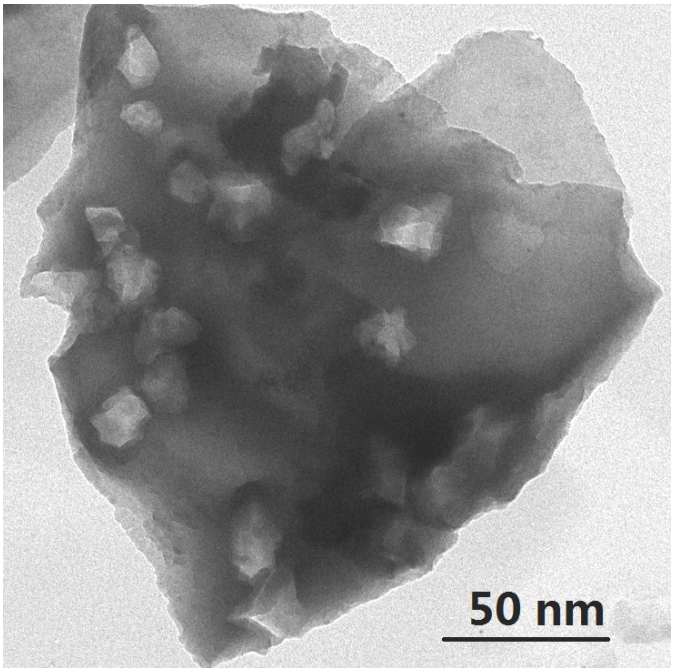

Fig. S15. High-resolution TEM image of the NC nanosheet without CuO and CoO obtained by the as-prepared NC@CoO/CuO soaked in dilute hydrochloric acid, then washed using water and dried.

Table S1 MOF-derived catalysts for OER

Catalyst	MOF used	Electrolyte	η_{10} (mV)	Tafel slope [mV ec^{-1}]	Ref.
NC@CoO/CuO	Cu(II)-Asp@Co(II)	0.5 M	272	67	present

nanosheets	nanofibers	KOH			work
Zn-doped $CoSe_2$/CFC	Zn, Co–ZIF	1 M KOH	356	88	S1
Co–MOF@CNTs	$Co(PhIm)_2 \cdot (DMF) \cdot (H_2O)$	1 M KOH	340	69	S2
Co–CNT–PC	ZIF-67	0.1 M KOH	315	73.8	S3
Co_3O_4C–NA	Co-naphthalenedicarboxylate	0.1 M KOH	290	70	S4

η_{10}–overpotential at current densities of 10 $mA \cdot cm^{-2}$

Table S2 Nanosheet-based catalysts for OER

Catalyst	Precursor	Electrolyte	Electrochemical performance	Ref.
NC@CoO/CuO nanosheets	Cu(II)-Asp@Co(II) nanofibers	0.5 M KOH	Overpotential and potential at current density of 10 $mA \cdot cm^{-2}$: 272 mV and 1.52 V vs. RHE, Tafel slope: 67 $mV \cdot dec^{-1}$	Present study
NiFe LDH/N-doped graphene	Graphene	0.1 M KOH	Overpotential at current density of 10 $mA \cdot cm^{-2}$: 337 mV	S5
Co–Bi/graphene	Graphene	1 M KOH	Overpotential at current density of 10 $mA \cdot cm^{-2}$: 290 mV	S6
P/N co-doped grapheme carbon nanosheets	Graphene, polyaniline	0.1 M KOH	Potential at 10 $mA \cdot cm^{-2}$: 1.57 V vs. RHE	S7
N/P/F tri-doped graphene	Graphene	0.1 M KOH	Tafel slope: 136 $mV \cdot dec^{-1}$	S8

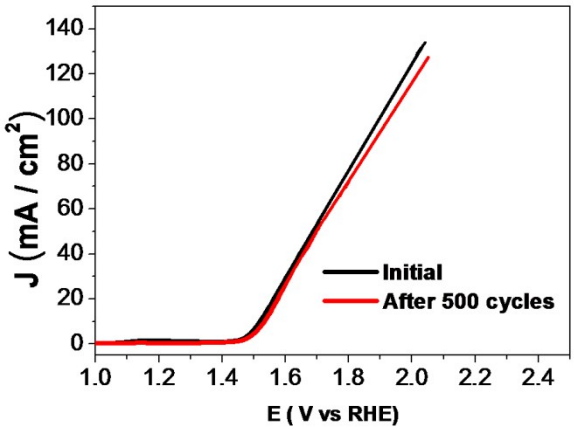

Fig. S14. Polarization curves of NC@CoO/CuO after 500 cycles.

References

S1. Q. Dong, Q. Wang, Z. Dai, H. Qiuand X. Dong, *ACS Appl. Mater. Interfaces,* 2016, **8**, 26902.

S2. Y. Fang, X.Li, F. Li, X. Lin, M. Tian, X. Long, X. An, Y. Fu, J. Jinand J. Ma, *J. Power Sources,* 2016, **326**, 50.

S3. S. Dou, X. Li, L. Tao, J. Huoand S. Wang, *Chem. Commun.,*2016, **52**, 9727.

S4. T. Y. Ma, S. Dai, M. Jaroniecand S. Z. Qiao, *J. Am. Chem. Soc.* 2014, **136**, 13925.

S5. C. Tang, H. S. Wang, H. F. Wang, Q. Zhang, G. L. Tian, J. Q. Nie, F. Wei, *Adv.Mater*. 2015, **27**,4516.

S6. P. Chen, K. Xu, T. Zhou, Y. Tong, J. Wu, H. Cheng, X. Lu, H. Ding, C. Wu, Y. Xie, *Angew.Chem. Int. Ed*. 2016, **55**,2488.

S7. R. Li, Z. D. Wei and X. L. Gou, ACS Catal., 2015, **5**, 4133.

S8. B. M. Hunter, J. D. Blakemore, M. Deimund, H. B. Gray, J. R. Winkler and A. M. Muller, *J. Am. Chem. Soc*., 2014, **136**, 13118.